The *Drosophila* Bub3 protein is required for the mitotic checkpoint and for normal accumulation of cyclins during G2 and early stages of mitosis

Carla S. Lopes[1], Paula Sampaio[1], Byron Williams[2], Michael Goldberg[2] and Claudio E. Sunkel[1,3,*]

[1]Instituto de Biologia Molecular e Celular, Universidade do Porto, Rua do Campo Alegre 823, 4150-180 Porto, Portugal
[2]Department of Molecular Biology and Genetics, Cornell University, Ithaca, NY 14853, USA
[3]Instituto de Ciências Biomédicas de Abel Salazar, Universidade do Porto, Largo do Prof. Abel Salazar n° 2, 4099-003 Porto, Portugal
*Author for correspondence (e-mail: cesunkel@ibmc.up.pt)

Accepted 20 October 2004
Journal of Cell Science 118, 187-198 Published by The Company of Biologists 2005
doi:10.1242/jcs.01602

Summary

During mitosis, a checkpoint mechanism delays metaphase-anaphase transition in the presence of unattached and/or unaligned chromosomes. This delay is achieved through inhibition of the anaphase promoting complex/cyclosome (APC/C) preventing sister chromatid separation and cyclin degradation. In the present study, we show that Bub3 is an essential protein required during normal mitotic progression to prevent premature sister chromatid separation, missegreation and aneuploidy. We also found that Bub3 is required during G2 and early stages of mitosis to promote normal mitotic entry. We show that loss of Bub3 function by mutation or RNAi depletion causes cells to progress slowly through prophase, a delay that appears to result from a failure to accumulate mitotic cyclins A and B. Defective accumulation of mitotic cyclins results from inappropriate APC/C activity, as mutations in the gene encoding the APC/C subunit cdc27 partially rescue this phenotype. Furthermore, analysis of mitotic progression in cells carrying mutations for *cdc27* and *bub3* suggest the existence of differentially activated APC/C complexes. Altogether, our data support the hypothesis that the mitotic checkpoint protein Bub3 is also required to regulate entry and progression through early stages of mitosis.

Supplementary material available online at
http://jcs.biologists.org/cgi/content/full/118/1/187/DC1

Key words: Drosophila, Mitosis, Checkpoint, Bub3, APC, Cyclosome

Introduction

During mitosis, a checkpoint mechanism delays entry into anaphase until all chromosomes are properly attached and aligned at the metaphase plate, thus preventing the unequal segregation of genetic material (Skibbens and Hieter, 1998). Genetic screens in budding yeast for mutants that do not arrest in mitosis after the induction of spindle damage allowed the identification of several components of this checkpoint. These include the Mad1, Mad2 and Mad3 proteins, the Bub1, Bub2 and Bub3 proteins and the kinase Mps1 (Hoyt et al., 1991; Li and Murray, 1991; Weiss and Winey, 1996). Soon after, homologues of most of these proteins were identified in higher eukaryotes, including Bub1, Bub3, Mad1, Mad2 and the human/mouse homologue of Mad3, BubR1; these proteins were further shown to localize preferentially to unattached kinetochores (Musacchio and Hardwick, 2002).

A biochemical link between the checkpoint and known regulators of mitotic progression first emerged from studies showing that the *Xenopus* and human homologues of Mad2 are able to bind and sequester Cdc20/Fizzy, an activator of the APC/C (Amon, 1999; Musacchio and Hardwick, 2002; Shah and Cleveland, 2000). The APC/C is a multi-subunit E3 ubiquitin ligase that targets several mitotic regulators, including securin and mitotic cyclins, for degradation by the proteasome, thus triggering mitotic exit. The APC/C subunits and many of its target proteins are present throughout the cell cycle, but APC/C activity and specificity towards the substrates is modulated by its association with co-factors such as Cdc20/Fizzy and Cdh1/Fizzy-related. APC/C association with Cdc20 occurs upon entry into mitosis and requires the phosphorylation of APC/C subunits. These phosphorylation events are thought to be mediated by cdc2/cyclin B and Polo kinases, and enhance the activity of the APC/C^{Cdc20} towards its substrates. The activity of APC/C^{Cdc20} triggers the metaphase-anaphase transition both by inducing the ubiquitination of securin and by targeting cyclin B for degradation. Cdh1, another co-factor, mediates the ability of the APC/C to degrade mitotic regulators, like polo and aurora kinases, and to degrade cyclin B completely, thus promoting mitotic exit. The interaction of the APC/C with Cdh1 is inhibited by Cdh1 phosphorylation, which is mediated by Cdk1 and Cdk2. As a result of cyclin B destruction, Cdk activity drops, ensuring that Cdh1 remains dephosphorylated and active, thus preventing the accumulation of mitotic cyclins during the subsequent G1 (Harper et al., 2002; Peters, 2002; Zachariae and Nasmyth, 1999). However, the G1/S transition and the G2 stage of the cell cycle require accumulation of cyclins A and B and therefore APC/C^{Cdh1} inactivation. The mechanism by which

the APC/C is regulated during these stages of cell cycle is still poorly understood. Recently it was found that APC/C inactivation during the G1/S transition is achieved by Emi1, a newly identified inhibitor of the APC/C, as well as by phosphorylation of Cdh1 by Cdks (Hsu et al., 2002; Reimann et al., 2001a; Reimann et al., 2001b).

The downstream target of the mitotic checkpoint is APC/C^{Cdc20}, whose inhibition prevents sister chromatid separation. However, the role of the various checkpoint components in APC/C inhibition has been a matter of some controversy. Not only Mad2, but also Mad3/BubR1 can interact directly with Cdc20 (Hardwick et al., 2000; Tang et al., 2001; Wu et al., 2000). Sudakin and colleagues purified an APC/C^{Cdc20} inhibitory complex from interphase cells, called the mitotic checkpoint complex (MCC), and showed that it contains Mad2, BubR1, Bub3 and Cdc20 (Sudakin et al., 2001). A similar complex was found in budding yeast and shown to be independent of kinetochore assembly (Fraschini et al., 2001; Hardwick et al., 2000). Tang and colleagues obtained similar results showing that a BubR1-containing complex was a stronger inhibitor of the APC/C^{Cdc20} than was Mad2, although this complex contained only BubR1 and Bub3 (Tang et al., 2001). Despite the discrepancies relative to the constitution of the complexes, these results suggest that checkpoint proteins may exist as APC/C inhibitory complexes already in interphase, however, the function of these complexes before mitosis is not yet known.

Even though most checkpoint components are strongly conserved through evolution, the role of some checkpoint proteins, in the checkpoint response is still unknown, particularly in the case of Bub3. Besides its association with BubR1 and Mad2 during interphase, Bub3 was also found in two independent complexes with Bub1 and BubR1 in mitotic mammalian and *Xenopus* cells (Campbell and Hardwick, 2003; Taylor et al., 1998); and was shown to be required for the localization of the mammalian proteins to the kinetochores (Taylor et al., 1998). In yeast, Bub3 was also found in a complex with Mad1 and Bub1; the formation of this complex is dependent on Mad2 and seems essential for the checkpoint response (Brady and Hardwick, 2000).

In order to study the function of Bub3 further, we searched for mutant alleles in *Drosophila* and carried out depletion of the protein in S2 cells. Our data show that Bub3 has an additional role besides its involvement in a checkpoint dependent mitotic arrest upon spindle damage. We report here that Bub3 is necessary to prevent APC/C-dependent degradation of mitotic cyclins during G2, thereby regulating both entry and transit through the initial stages of mitosis. Furthermore, our data suggest the existence of differentially activated APC/C complexes, which are inhibited by Bub3 to ensure accumulation of mitotic cyclins.

Materials and Methods

Fly stocks

Df (3R)Dr-rv1 (breakpoints 99A01-02; 99B06-11) and *cdc27* $^{l(3)L7123}$ were obtained from the Bloomington (IN) Stock Center. To rescue the *bub3*^{1} mutation, a full-length *bub3* cDNA was cloned into the pP{UAST} vector (Brand and Perrimon, 1993), injected into *w*^{1118} embryos and a number of stable transformants were obtained. To activate transcription of the transgene, p{UAST-*bub3*}; *bub3*^{1}/TSTL individuals were crossed with a strain carrying Mz1061 and the *bub3*^{1} mutation. The resulting ({pUAST-bub3}/+; *bub3*^{1}/*bub3*^{1}) flies were viable and no mitotic phenotype was observed. A non-degradable form of cyclin B was expressed from the transgene p{UAS-CBTPM-GFP} (Wakefield et al., 2000). *bubR1*^{1} was described previously (Basu et al., 1999) (see also Logarinho et al., 2004).

Cytological analysis of *Drosophila* neuroblasts

Third instar larval brains were dissected, fixed and stained as previously described (Llamazares et al., 1991). Whenever required, brains were dissected in PBS and incubated in 10 μM colchicine (Sigma) for 1 hour prior to fixation. Mitotic index was defined as the number of mitotic cells per optical field, with every optical field in the brain being scored. Immunostaining of neuroblasts from third instar larvae was performed as previously described (Platero et al., 1995). Anti-Bub3 antibody (Logarinho et al., 2004) was diluted 1:500, anti-Polo antibody (Llamazares et al., 1991) diluted 1:50 and anti-cyclin B antibody (Jacobs et al., 1998) was used at 1:3000 dilution. For analysis of cyclin B levels, all images were acquired using the same parameters in a Zeiss Axioscop microscope with a SPOT 2 camera (Diagnostic Instruments, USA). Quantification of cyclin levels per cell was carried out using ImageJ 1.30v software (http://rsb.info.nih.gov). The mean pixel intensity per cell area for different genotypes at different stages of the cell cycle was determined and used for further statistical analysis (Student's *t*-test). Cyclin levels in at least five brains were scored for each genotype.

DsRNA interference in *Drosophila* S2 cells

To deplete Bub3 from S2 cells, a fragment of 600 bp spanning the 5′ UTR of *bub3* and including the ATG initiation codon was cloned into the vectors pSPT18 and pSPT19 (Roche). RNA was synthesized using the T7 Megascript kit (Ambion). 15 μg dsRNA were added to 10^{6} *Drosophila* S2 cells in Schneider's medium (Gibco, BRL) and incubated for 1 hour, after which cells were supplemented with 2 ml media with 10% FBS (Gibco, BRL). Experiments were performed at least three times, in six-well plates and at each time point cells were collected and processed for immunofluorescence and immunoblotting. For immunoblotting, cells were collected by centrifugation, washed in PBS supplemented with protease inhibitors (Roche) and resuspended in 2× SDS-sample buffer before loading on a 12% SDS-PAGE. When required, cells were incubated with 30 μM colchicine (Sigma). Mitotic index was determined as the percentage of anti-phosphorylated histone H3 (PH3: Upstate Biotechnology)-positive cells.

Immunofluorescence in *Drosophila* S2 cells

Cells were centrifuged onto coverslips and fixed in 3.7% formaldehyde, 0.5% Triton X-100 in 1× PBS, for 8 minutes, followed by a washing step in 1× PBS, 0.1% Triton X-100 (PBST). Rabbit anti-PH3 (Upstate Biotechnology) was diluted to 1:1000, γ-tubulin (GTU88, Sigma) was diluted at 1:1500 and anti-cyclin A was diluted to 1:4000 (Whitfield et al., 1990). Anti-rabbit Alexa 488 and anti-mouse Alexa 568 (Molecular Probes), were used as secondary antibodies. DNA was counterstained with DAPI in Vectashield (Vector, UK). All images were collected, deconvolved and projected using Cell Observer System (Zeiss, Germany). Adobe Photoshop 7.0 (Adobe Systems) was used to process all images.

Western blotting

Third instar larvae brains were dissected and homogenized at 4°C in 1× PBS supplemented with protease inhibitors (Roche Diagnostics). 10-40 μg of total protein extracts were resolved in 10-12% SDS-PAGE and transferred to nitrocellulose membrane (Schleicher and Schuell). Immunopurified anti-Bub3 was diluted 1:50 in PBST

containing 1% BSA. α-tubulin was detected using mAb B512 (Sigma) diluted 1:5000. Anti- cyclin B antibody was diluted at 1:10,000. Secondary antibodies conjugated to HRP (Vector, UK) were used according to the manufacturer's instructions.

Time-lapse fluorescence imaging

Live analysis of mitosis was done on S2 cells stably expressing GFP-tubulin. Control or Bub3 RNAi-treated cells were incubated for 96 hours and plated on glass coverslips treated with 30 μg/ml concanavalin A (Sigma). Time-lapse images were collected at 2 minute intervals, starting from the time asters could be visualized, using a Cell Observer System (Zeiss, Germany). Image sequence analysis and movie assembly was done with ImageJ Software (NIH, USA) and Quicktime 6 (Apple Computer, USA). The time between the appearance of the asters and the nuclear envelope breakdown, as well as the beginning of anaphase was determined and used for further statistical analysis (Student's *t*-test).

Results

Characterization of a new *bub3* mutant allele

During a search for *Drosophila* genes involved in the regulation of mitotic progression, we isolated a recessive mutant line in which the lethality mapped to the *bub3* locus. Genomic sequencing of the *bub3* gene in this line showed that it contained a single point mutation in the coding region, leading to the substitution of a conserved glycine at position 193 by aspartic acid (data not shown). This mutation is responsible for the lethality of the line, as expression of wild-type *bub3* cDNA during larval development using a specific

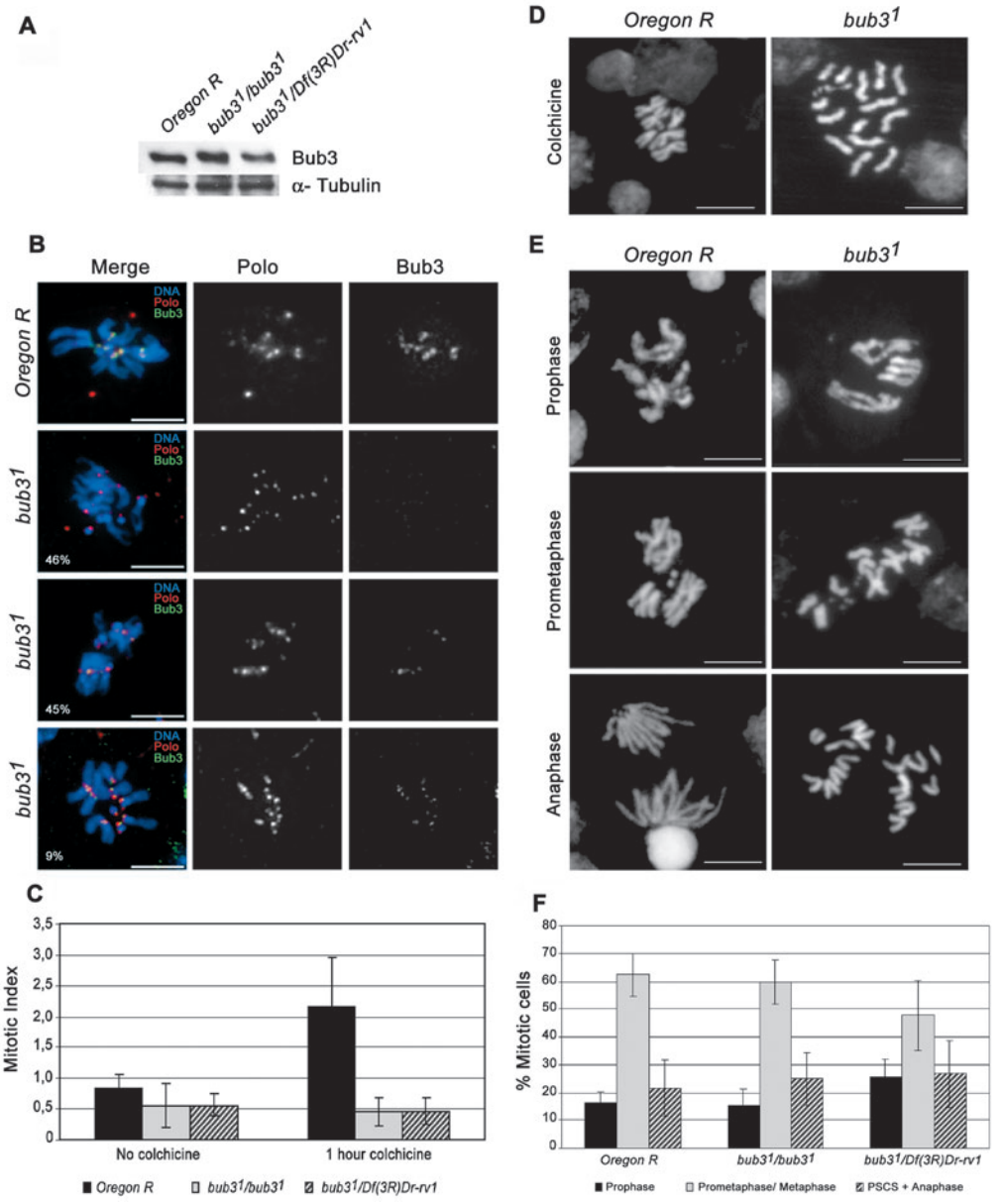

Fig. 1. Mutations in *bub3* result in premature sister chromatid separation, abnormal anaphase and aneuploidy. (A) Western blot of total protein extracts from wild-type (*Oregon R*), *bub3*^{1} homozygous and *bub3*^{1}*/Df(3R)Dr-rv1* neuroblasts with anti-Bub3 antibody. α-tubulin was detected as a loading control. (B) Immunolocalization of Bub3 in wild-type and *bub3*^{1} mutant neuroblasts (*n*=354) showing that the Bub3 mutant protein fails to localize to kinetochores in 46% of the mitotic cells. In 45% of the prometaphases of *bub3*^{1} mutant cells, Bub3 can localize to some kinetochores, whereas in only 9% of prometaphases is Bub3 detected with reduced intensity at all kinetochores. Polo was used to label kinetochores. DNA is shown in blue, polo in red and bub3 in green in the merged image. (C) Mitotic index of third instar larvae neuroblasts from *Oregon R*, *bub3*^{1}*/bub3*^{1} and *bub3*^{1}*/Df(3R)Dr-rv1*, after a 1 hour incubation in colchicine. *bub3*^{1} mutant cells fail to sustain mitotic arrest upon spindle damage. (D) Squashed preparations of wild-type and *bub3*^{1} neuroblasts after incubation in colchicine. Upon spindle damage, *bub3*^{1} mutant cells fail to maintain sister chromatid cohesion. (E) Squashed preparations of wild-type and *bub3*^{1} mutant larvae neuroblasts at different stages of mitosis. *bub3*^{1} mutant neuroblasts show aneuploidy, PSCS and anaphases with lagging chromatids. (F) Quantification of mitotic parameters in *Oregon R*, *bub3*^{1} homozygous and *bub3*^{1}*/Df(3R)Dr-rv1* third instar larvae neuroblasts, showing that homozygous and hemizygous cells behave differently during the initial stages of mitosis. Bar, 5 μm.

GAL4 driver rescues the mitotic phenotype and gives rise to viable adults. Thus, in *Drosophila*, *bub3* is an essential gene and we have designated this mutant allele *bub3*^{1}. Western blot analysis of total protein extracts from *bub3*^{1} homozygous or *bub3*^{1}*/Df(3R)Dr-rv1* hemizygous individuals indicates that the mutant protein is expressed (Fig. 1A). To evaluate whether the mutant protein is able to localize properly, antibodies were used to determine its intracellular localization in *bub3*^{1} third instar larvae neuroblasts. Although in wild-type cells Bub3 always localizes to kinetochores during prometaphase, in approximately half *bub3*^{1} cells the mutant protein is not detected at kinetochores (Fig. 1B). However, some *bub3*^{1} cells (45%) show localization of the mutant protein at one or two kinetochore pairs, whereas only very few (9%) show localization to all kinetochores, suggesting that this allele might behave as a hypomorph.

To determine whether *bub3*^{1} cells have an abnormal mitotic checkpoint response, we measured the mitotic index of both *bub3*^{1} homozygous and hemizygous neuroblasts in the presence and absence of spindle damage (Fig. 1C and supplementary material Table S1). The results show that in the absence of spindle damage, the mitotic index of mutant larvae is not significantly different from wild-type controls. However, if the spindle is disrupted by colchicine, neither *bub3*^{1} homozygous nor hemizygous mutant cells are able to arrest in mitosis and undergo precocious sister chromatid separation (PSCS) (Fig. 1C,D and supplementary material Table S1) indicating loss of mitotic checkpoint response.

We next examined mitotic progression in both homozygous and hemizygous mutant individuals. As the phenotype associated with both genotypes is nearly identical, only observations on homozygous mutant cells are shown (Fig. 1E). *bub3*^{1} mutant cells undergo cytologically normal prophase but, a significant proportion of cells with a prometaphase-like

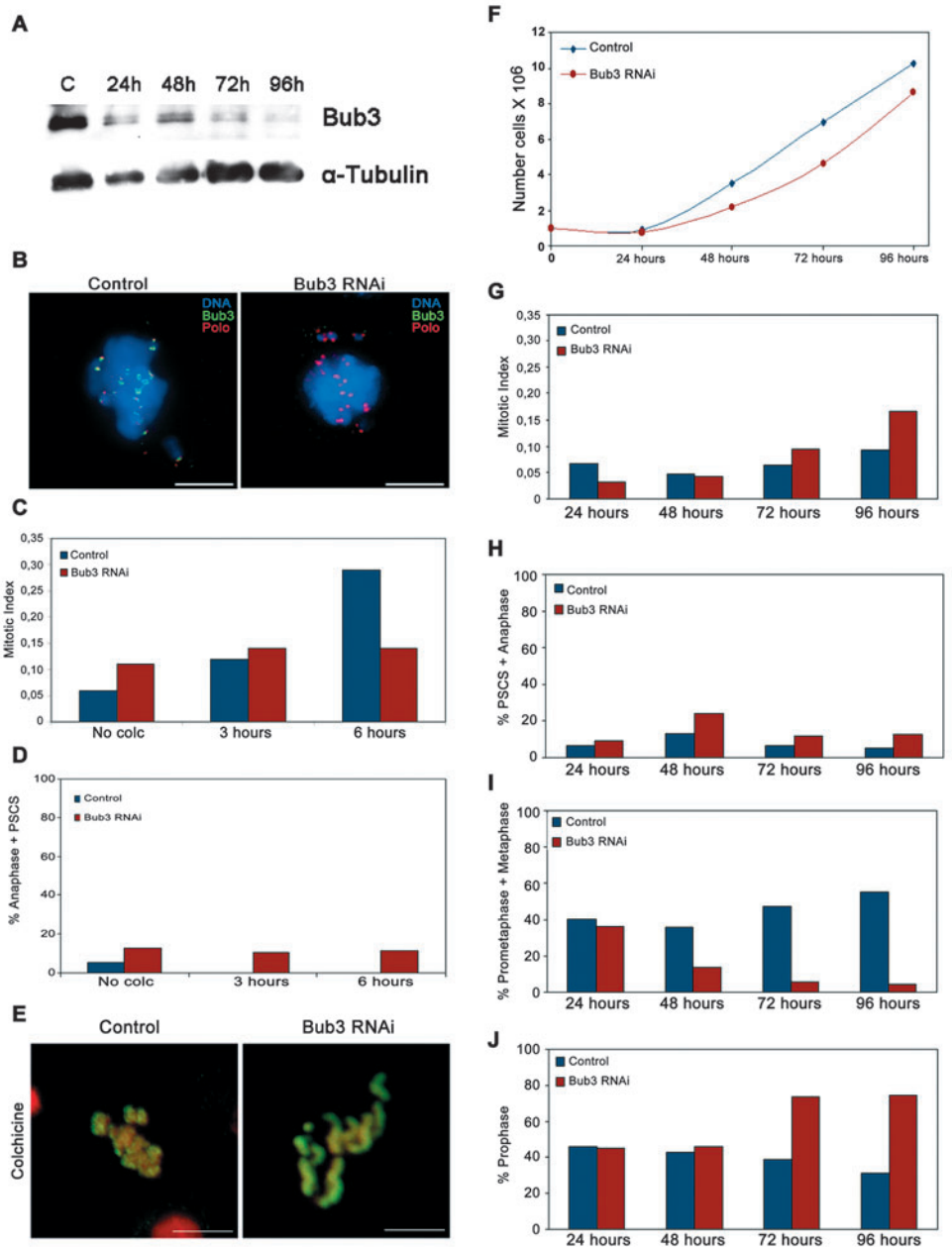

Fig. 2. Depletion of Bub3 in *Drosophila* S2 cells results in slower progression through prophase and premature exit from mitosis. (A) Western blot showing depletion of Bub3 after RNAi at different times. α-tubulin antibody was used as loading control. (B) Immunolocalization of Bub3 in control and Bub3 dsRNA-treated cells, after 96 hours in culture. Polo was used to label kinetochores. Merged images are shown with DNA in blue, polo in red and bub3 in green. (C) Mitotic index of control and S2 cells treated with Bub3 dsRNA for 96 hours after incubation in colchicine for different times. Mitotic index was determined as the number of phospho-histone H3 (PH3)-positive cells over the total cell population. (D) Percentage of mitotic cells showing sister chromatid separation (SCS, anaphases plus PSCS) after incubation with colchicine, in control and Bub3-depleted cells. (E) RNAi-treated Bub3 cells showing SCS after incubation with colchicine. DNA is shown in red and PH3 in green. (F) Proliferation rate of control and Bub3 RNAi-treated cells. (G) Time course analysis of the mitotic index after Bub3 RNAi, assessed by PH3 staining. (H-J) Analysis of mitotic progression of control and S2 cells treated with RNAi. Mitotic cells were identified by immunostaining with PH3 specific antibodies. (H) Quantification of cells in anaphase and prometaphase-like cells in which sister chromatids are clearly separated over time. (I) Treatment of S2 cells with Bub3 RNAi reduces the number of cells in prometaphase and metaphase over time. (J) Depletion of Bub3 causes a marked increase in the number of cells in prophase by 72 hours after treatment. Bar, 5 μm.

configuration (19%) display PSCS. Furthermore, most of the anaphases (70%) observed are disorganized and contain lagging chromatids, and of the total mitotic figures a high proportion (38-42%) are aneuploid, probably reflecting the occurrence of PSCS in prior rounds of cell division.

Although our observations of late mitotic stages indicated that *bub3*^{1} homozygous and hemizygous mutant cells had nearly identical phenotypes, the two genotypes behave differently during the early stages of mitosis (Fig. 1F and supplementary material Table S1). Although the frequency of prophase and prometaphase cells in *bub3*^{1} homozygous mutants does not differ significantly from the wild type, hemizygous individuals have a higher frequency of cells in prophase and a correspondingly lower frequency of cells in prometaphase. This classical genetic test verifies our previous conclusion from cytological analysis that the *bub3*^{1} allele behaves as a hypomorph. Importantly, these results further suggest that a more severe depletion of Bub3 function causes a slow progression through early stages of mitosis, a phenotype that to our knowledge has not been described before for any checkpoint protein.

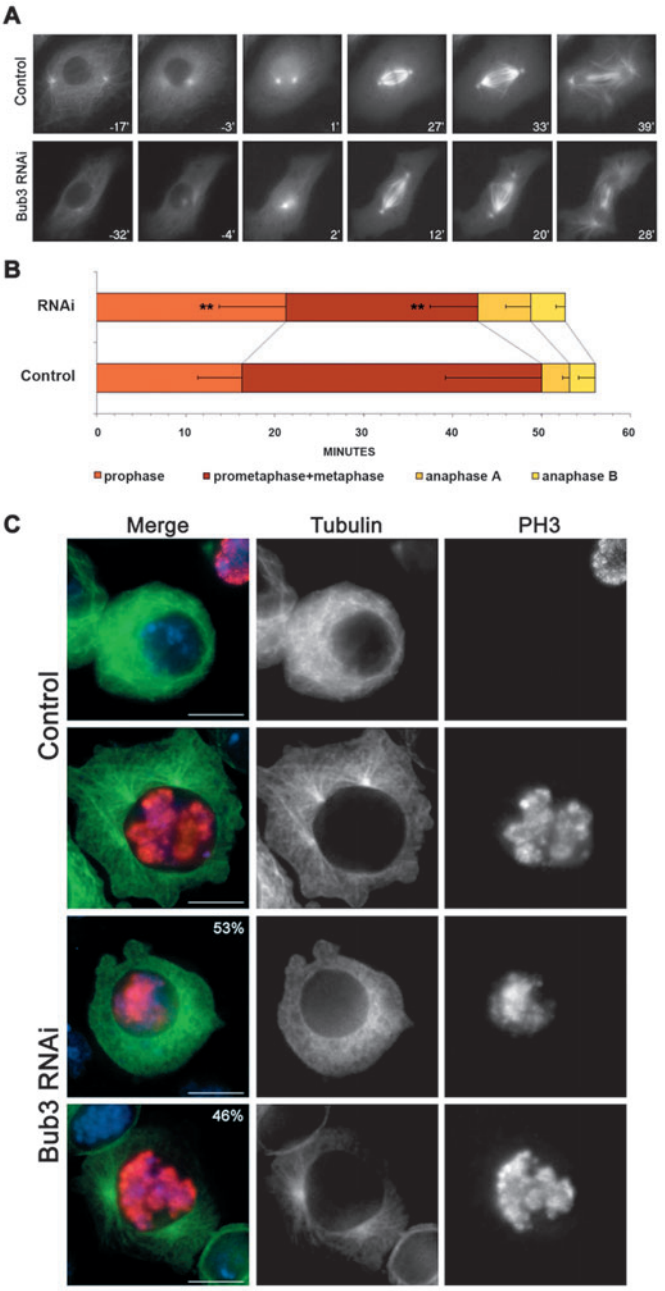

Mitotic progression after depletion of Bub3 in *Drosophila* S2 cells

The results above suggest an unexpected role for Bub3 during early mitotic stages that only became apparent in *bub3*^{1} hemizygous individuals. We therefore proceeded to analyse the consequences of depleting Bub3 in *Drosophila* S2 cells by double-stranded RNA interference (RNAi). Treatment of S2 cells with *bub3* RNAi (Fig. 2) caused a significant reduction of the Bub3 protein levels within 48 hours and by 96 hours the protein was barely detectable (Fig. 2A). Immunofluorescence analysis on RNAi-treated cells failed to detect Bub3 at kinetochores in all mitotic cells examined (Fig. 2B and data not shown). Accordingly, Bub3-depleted cells are unable to arrest in mitosis when the spindle is damaged (Fig. 2C), and show elevated levels of PSCS (Fig. 2D,E). Similar to the results presented above for *bub3*^{1} mutant neuroblasts, depletion of Bub3 by RNAi demonstrates that in *Drosophila* S2 cells, Bub3 is required for an efficient mitotic checkpoint response.

We next addressed the role of Bub3 in mitotic progression. Depletion of Bub3 causes a reduction in cell proliferation (Fig. 2F) that is not due to loss of cell viability (data not shown), but instead to an increase in the culture doubling time. Quantification of the mitotic index over the course of the experiment shows that in comparison with control cells, the number of cells in mitosis increases after depletion of Bub3 (Fig. 2G). These results contradict a role for Bub3 as a negative regulator of mitotic exit and suggest that Bub3-depleted cells spent more time in mitosis, leading to a slower proliferation rate. To better understand this unexpected behaviour, we carefully analysed mitotic progression. The results show that depletion of Bub3 leads to an increase in the number of cells with PSCS (Fig. 2H). Compared to control cells, there is also a twofold increase in the total number of cells in anaphase and

Fig. 3. In vivo analysis of S2 cells shows that Bub3-depleted cells transit faster through mitosis, despite a delay in prophase.
(A) Selected images from time-lapse movies (see supplementary material Movie 1) of either control or Bub3 RNAi-treated cells expressing GFP-tubulin recorded every 2 minutes from the time asters first appeared to the re-formation of the daughter nuclei. The two movies have been aligned setting nuclear envelope breakdown (NEBD) as 0. In control cells, NEBD occurred approximately 17 minutes after asters were clearly visualized, whereas anaphase started 32 minutes after NEBD. In Bub3 RNAi-treated cells, NEBD occurred 32 minutes after aster formation, showing a significant delay in prophase. Anaphase started approximately 20 minutes after NEBD, indicating a rapid transition from prometaphase to anaphase.
(B) Quantitative analysis of the different cell cycle stages, in both control (n=14) and Bub3 RNAi-treated cells (n=29). $^{**}P<0.005$ when compared to corresponding stages in control cells.
(C) Analysis of prophase cells by PH3 labelling reveals that the majority of the Bub3-depleted cells (53%) exhibits strong PH3 labelling and DNA condensation but no aster formation, in contrast to the control population where PH3 staining correlated with aster formation in more than 98% of cells (n=40).

most anaphases (68%) are disorganized or have lagging chromatids (data not shown). Notably, after depletion of Bub3 there is a significant reduction in the number of cells in prometaphase and metaphase, whereas approximately 57% of the prometaphase cells exhibit PSCS (Fig. 2I). These data are all consistent with a premature mitotic exit. If these cells exit mitosis earlier than normal, then the higher mitotic index observed after depletion of Bub3 (Fig. 2G) must result from a delay at an earlier stage of mitosis. Indeed, there is a twofold increase in the percentage of cells in prophase 72 hours after treatment with RNAi (Fig. 2J). Therefore, a severe depletion of Bub3 in S2 cells results in mitotic alterations similar to those observed in *bub3*^{1} hemizygous neuroblasts. Both sets of observations indicate that besides its function in the mitotic checkpoint response, Bub3 has a role in promoting normal transit through early stages of mitosis, particularly through prophase.

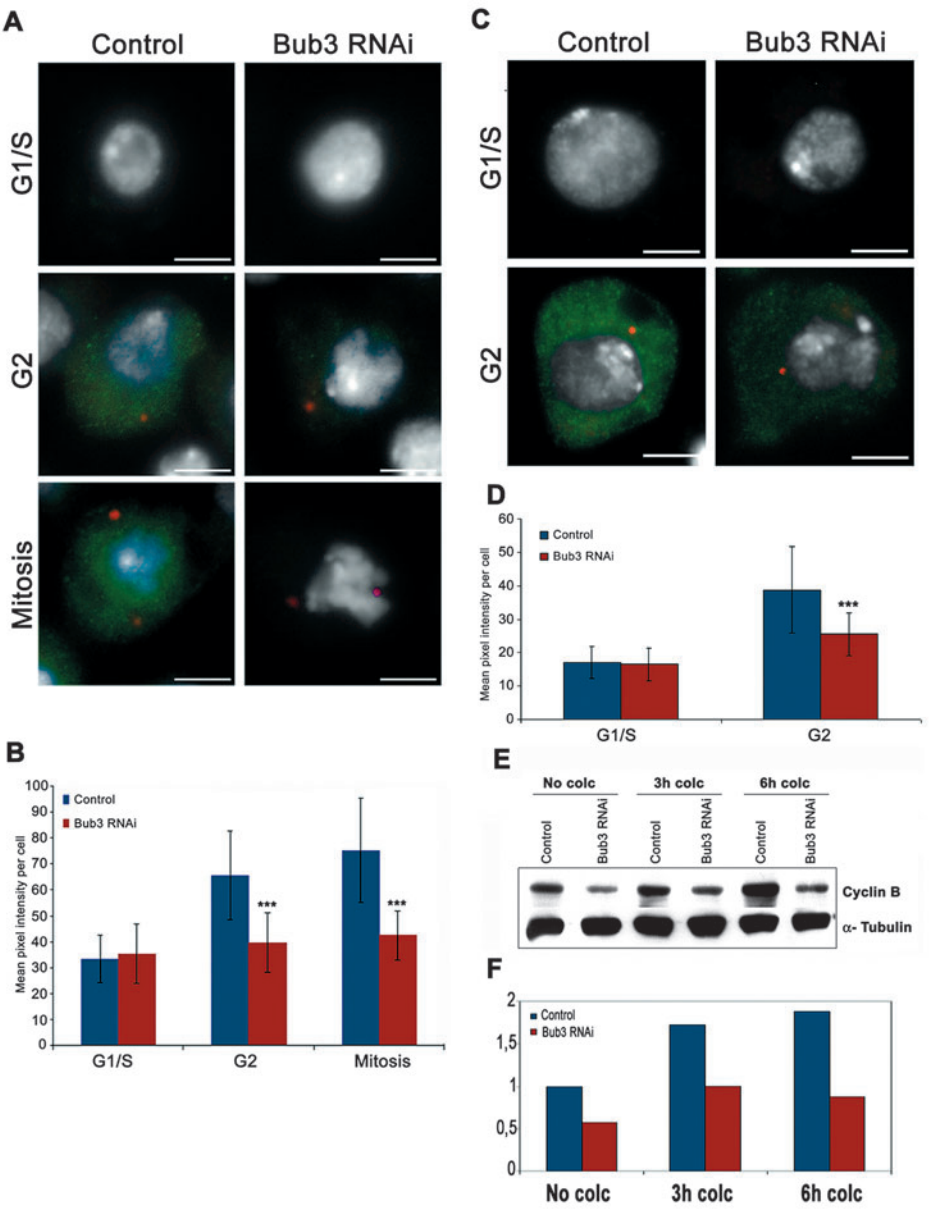

Fig. 4. Bub3-depleted cells exhibit lower levels of cyclin B during G2 and mitosis. (A) Analysis of cyclin B at different stages of the cell cycle in control and Bub3 RNAi-treated cells for 96 hours, followed by incubation for 6 hours in colchicine. γ-tubulin staining (red) was used to discriminate between G1/S, G2 and mitotic cells. DNA is shown in white and cyclin B in green. Images show that Bub3-depleted cells do not accumulate cyclin B to control levels in G2 or during mitosis. (B) Quantification of cyclin B levels. The mean pixel intensity per cell in control and RNAi-treated cells was measured at different cell cycle stages (see also supplementary material Table S2). ***P<0.0005 when compared to intensity in control cells. (C) Cyclin B accumulation during G1/S and G2 in control and Bub3-depleted cells after 96 hours in culture without colchicine treatment. γ-tubulin staining (red) was used to classify cells as before, cyclin B is shown in green and DNA in white. Bub3-depleted cells fail to accumulate cyclin B during G2, unlike control cells. (D) Quantification of cyclin B levels (see also supplementary material Table S3). ***P<0.0005 when compared to intensity in control cells. (E) Analysis of cyclin B levels by western blotting of total protein extracts (10 μg) isolated from control or RNAi-treated cells before or after 3 and 6 hour incubations with colchicine. α-tubulin was detected as a loading control. (F) Quantitative analysis of the western blot shown in E. Bar, 5 μm.

In vivo analysis of cell division after depletion of Bub3

To clarify further a possible role of Bub3 in mitotic progression, we performed in vivo time-lapse analysis of S2 cells stably expressing GFP-tubulin after depletion of Bub3 by RNAi. Control and Bub3-depleted cells were recorded every 2 minutes from the time asters first appeared to the re-formation of the daughter nuclei. GFP-tubulin is an excellent marker to follow mitotic progression, as we can time various events. The visualization of well-defined asters was taken to indicate initiation of prophase, nuclear envelope breakdown (NEBD) can be seen by rapid entry of GFP-tubulin into the nuclear area, retraction of kinetochore bundles shows the beginning of anaphase A, spindle elongation marks anaphase B and nuclear re-formation indicates telophase. Thus, we can determine the duration of all major mitotic phases including prophase (from appearance of the asters until NEBD), prometaphase-metaphase (from NEBD until anaphase initiation), anaphase A (from microtubule bundle retraction to spindle elongation) and anaphase B (from spindle elongation to nuclear reformation) allowing a direct correlation between the in vivo data and results from fixed material. The results show that depletion of Bub3 causes significant changes in mitotic progression during both prophase and prometaphase (Fig. 3 and

supplementary material Movies 1 and 2). The appearance of the asters was set as time zero, and the duration of each mitotic stage was plotted (Fig. 3A,B). In vivo analysis of untreated S2 cells shows that prophase takes on average 16 minutes, however, after Bub3 depletion, prophase is significantly delayed lasting on average 21 minutes (Fig. 3A,B and supplementary material Movies 1 and 2). Furthermore, although in control cells the timing between NEBD and anaphase onset takes on average 34 minutes (Fig. 3A,B and supplementary material Movie 1), after Bub3 depletion it is significantly reduced to 21 minutes on average, indicating an accelerated progression through prometaphase-metaphase. These data are in agreement with the proposed function of Bub3 in the mitotic checkpoint response.

Thus, depletion of Bub3 causes a significant delay in prophase, strongly supporting our observations in fixed cells (see above). However, we were surprised not to find a more significant prophase delay as depletion of Bub3 causes a twofold increase in the percentage of cells in prophase (Fig. 2J). To clarify this discrepancy, the number cells in prophase, in S2 cells expressing GFP-tubulin after Bub3 RNAi was quantified using PH3 as a mitotic marker. Two hallmark events of prophase were analysed: the appearance of PH3 at Ser10, which in *Drosophila* correlates with the beginning of prophase (Hendzel et al., 1997) and separation of the centrosomal asters. This analysis also showed a twofold increase in the number of cells in prophase after Bub3 depletion as described previously (data not shown). However, unlike control cells, in Bub3 depleted cells, two types of PH3 positive cells were clearly observed: cells in which formation of the asters was markedly visible and cells with an interphase arrangement of microtubules without visible asters (Fig. 3C). The latter phenotype accounted for 53% of the prophase cells observed after Bub3 depletion and was never observed in control cells. In the control population, the appearance of the asters always correlated with PH3 staining. These observations suggest that the in vivo analysis is likely to underestimate the prophase delay observed after depletion of Bub3.

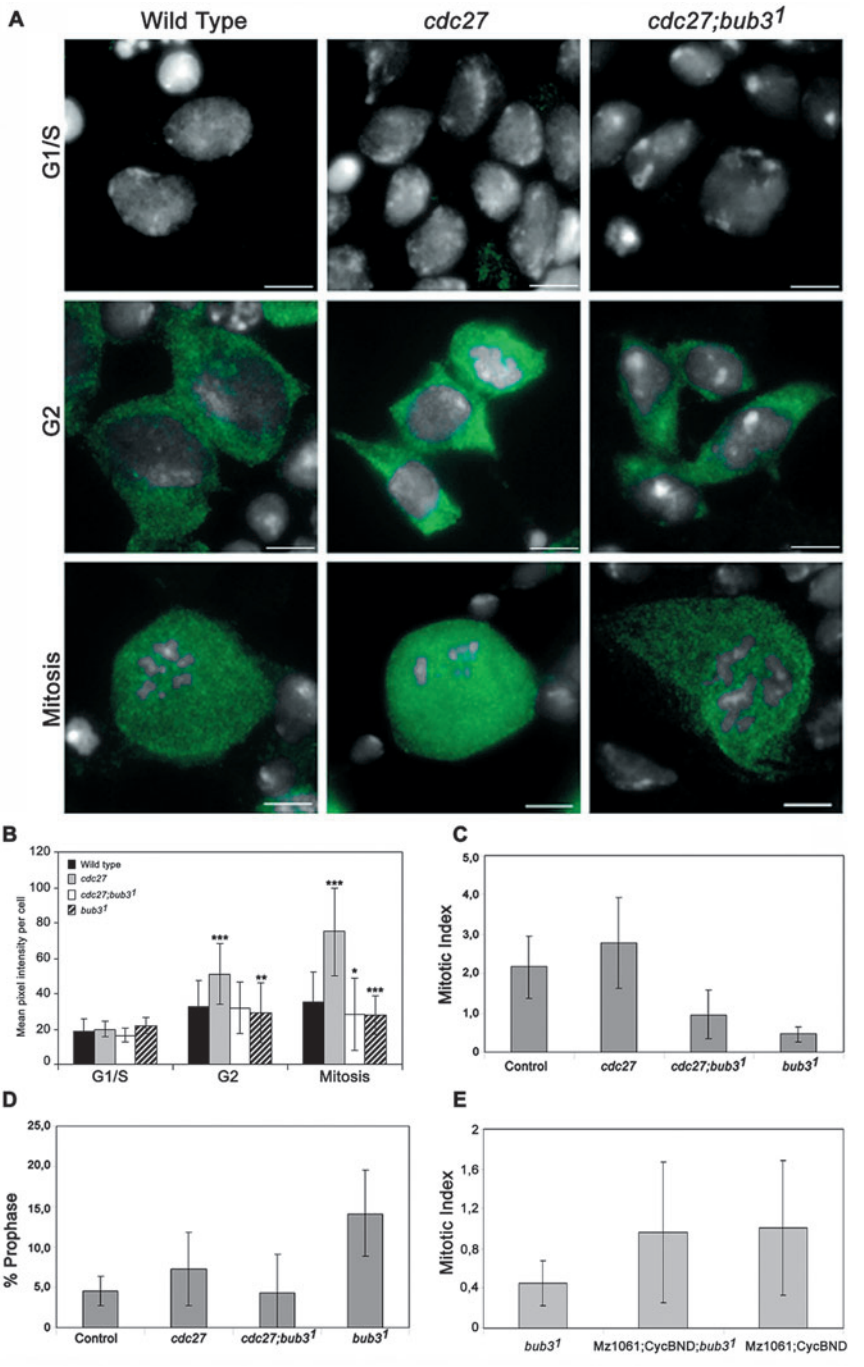

Fig. 5. Mutation of the APC/C subunit cdc27 in *bub3¹* mutant cells allows cyclin B accumulation during G2 and restores normal progression through early mitotic stages. (A) Neuroblasts of different genotypes were isolated, incubated in colchicine (1 hour), fixed and stained for cyclin B (green). DNA was counterstained with DAPI (white). Images show high levels of cyclin B in *cdc27* mutant cells whereas *cdc27;bub3¹* double mutant cells show normal cyclin B levels during G2. (B) Quantification of cyclin B levels. The mean pixel intensity per cell in the wild type and mutant strains at different cell cycle stages was measured (see also supplementary material Table S4). **P*<0.05; ***P*<0.005; ****P*<0.0005 when compared to intensity in corresponding control cells. (C) Mitotic index of wild-type (control), double mutant (*cdc27;bub3¹*) and single mutant (*cdc27* or *bub3¹*) cells. Mutation of *cdc27* in a *bub3¹* background leads to an increase in the mitotic index relative to *bub3¹* alone, but still reduced when compared to the wild-type index. (D) Quantification of cells in prophase for the different genetic backgrounds showing that double mutant cells (*cdc27; bub3¹*) transit normally through prophase. (E) A non-degradable form of cyclin B (CyCBND) was expressed in *bub3¹* mutant neuroblasts (Mz1061;CycBND-GFP;*bub3¹*). Mz1061 was used to drive neuroblast expression. Mz1061;CycBND-GFP neuroblasts were used as a control. Expression of a non-degradable form of cyclin B in *bub3¹* neuroblasts restores the mitotic index to wild-type values. Bar, 5 μm.

Analysis of cyclin B levels during G2 and mitosis in Bub3-depleted cells

The results described above suggest that after Bub3 depletion, nuclear and cytoplasmic events, namely chromosome condensation and spindle formation, appear to uncouple. It is well established that accumulation of mitotic cyclins and the activation of the cdk/cyclin complexes is essential for entry and progression through mitosis (Zachariae and Nasmyth, 1999). Besides being important for chromosome condensation (Kimura et al., 1998) cdk activity is responsible for the dramatic changes in microtubule dynamics that occur at the onset of mitosis, resulting in microtubule nucleation from centrosomes and assembly of the mitotic spindle (Buendia et al., 1992; Verde et al., 1992). Accordingly, we next tested whether the slower progression through early mitotic stages observed after Bub3 depletion could result from abnormal accumulation of mitotic cyclins. Cyclin B levels were measured by immunofluorescence and western blot analysis in cells that had been depleted of Bub3 by RNAi (Fig. 4). Control and RNAi-treated cells were incubated in colchicine, to promote high levels of cyclin accumulation and increase the number of cells in mitosis, and cyclin B levels were measured by immunofluorescence (Fig. 4A,B). The centrosomal marker γ-tubulin was used to distinguish between different cell cycle stages. Interphase cells without γ-tubulin staining were classified as G1/S, whereas those with centrosomal staining but without centrosome separation were classified as G2. Cells in mitosis (prophase and prometaphase) had γ-tubulin staining, well-separated centrosomes and clear chromosome condensation (Fig. 4A). The fluorescence intensity values obtained for G1/S cells did not differ between control and RNAi-treated cells (Fig. 4A,B and supplementary material Table S2) allowing a direct comparison between the two samples. In agreement with the expected pattern for cyclin B accumulation, S2 control cells start to accumulate cyclin B during G2 and attain their highest levels of cyclin B during mitosis (Fig. 4A,B and supplementary material Table S2). However, cyclin B accumulation in Bub3-depleted cells is surprisingly different. These cells already show significantly lower levels of cyclin B in G2 and also during mitosis. The

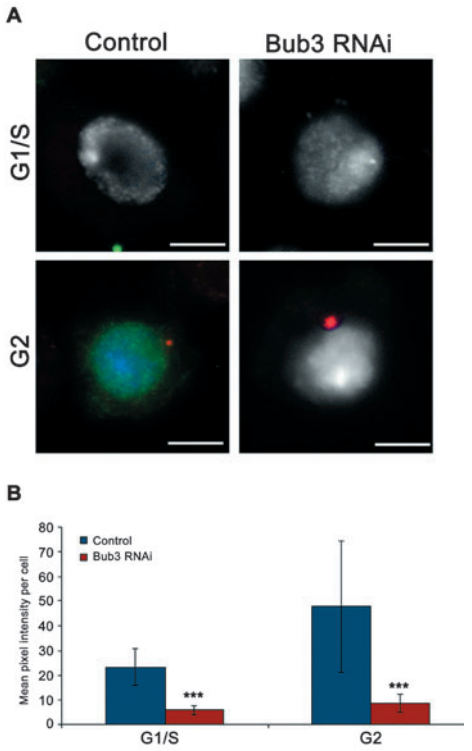

Fig. 6. Bub3 is required to promote accumulation of cyclin A during G2. (A) Cyclin A accumulation during G1/S and G2 in control and Bub3-depleted cells. γ-tubulin staining (red) was used to classify G1/S and G2 cells. Cyclin A is shown in green and DNA in white. Bub3-depleted cells fail to accumulate cyclin A in G2. (B) Quantification of cyclin A levels for control and RNAi-treated cells. Image analysis was performed as described for cyclin B and the mean pixel intensity per cell at the different stages of cell cycle was determined (see also supplementary material Table S6); ***P<0.0005 when compared to intensity in control cells. Bar, 5 μm.

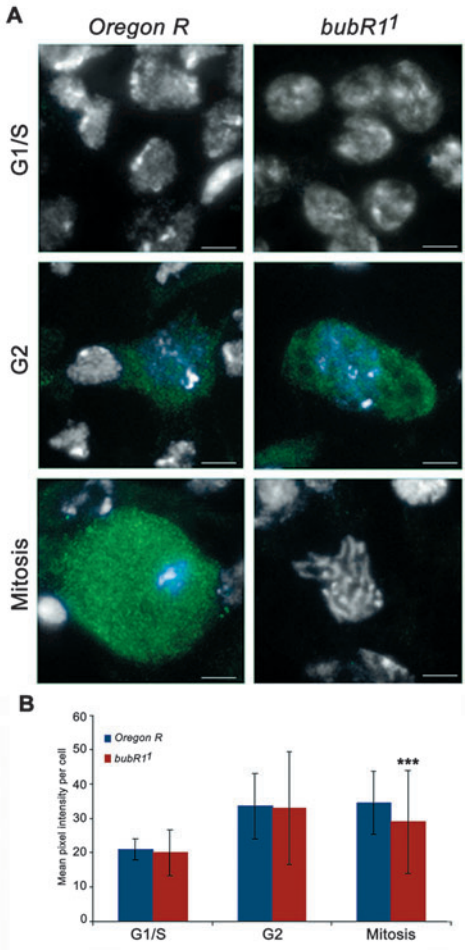

Fig. 7. Mutations in *bubR1*^{1} do not affect cyclin B accumulation during G2. (A) *bubr1*^{1} mutant neuroblasts were treated with colchicine as previously described, fixed and stained for DNA (white) and cyclin B (green). The results show that unlike *bub3*^{1}, *bubR1*^{1} mutant cells do not compromise accumulation of cyclin B during G2. Nevertheless, as expected, cyclin B levels during mitosis decrease significantly because of loss of spindle checkpoint activity. (B) Quantification of cyclin B levels at different cell cycle stages in *Oregon R* (wild-type strain) and *bubR1*^{1}, was performed as described for *bub3*^{1} (see also supplementary material Table S7). **P<0.005; ***P<0.0005 when compared to intensity in the relevant control cells. Bar, 5 μm.

failure to maintain high levels of cyclin B during mitosis is in agreement with the predicted function of Bub3 in the mitotic checkpoint response (similar results were also observed in *bub3*^{1} mutant neuroblasts: see supplementary material Fig. S1 and Table S2). However, these results also indicate that Bub3 might be required during G2 to ensure accumulation of cyclin B. To eliminate the possibility that colchicine treatment could indirectly affect cyclin B accumulation during G2, cyclin B levels were measured in control and Bub3-depleted cells in the absence of the drug (Fig. 4C,D). Quantification of cyclin B levels shows that in contrast to control cells, Bub3-depleted cells fail to accumulate cyclin B during G2 (Fig. 4D and supplementary material Table S3). In agreement with the immunofluorescence data, western blot analysis of total protein extracts shows that after Bub3 depletion, accumulation of cyclin B is significantly reduced reaching only 50% of the levels observed in untreated cells (Fig. 4E,F). In addition, although treatment with colchicine leads to accumulation of cyclin B in control cells, the same is not observed after Bub3 depletion, where accumulation of cyclin B is severely compromized. These results show that Bub3 does indeed appear to be required during G2 to promote accumulation of cyclin B, strongly suggesting that Bub3 might have a function in G2 before its well-established role in the mitotic checkpoint during prometaphase.

Analysis of cyclin B accumulation and mitotic progression in cells mutated for *bub3* and a subunit of the APC/C

Accumulation of cyclins during G2 in somatic cells depends primarily upon transcriptional activation and the fact that the anaphase promoting complex/cyclosome (APC/C) is inhibited at this stage by early mitotic regulators (Reimann et al., 2001a). To test whether APC/C activity might be required to mediate the reduction in cyclin B levels after depletion of Bub3, we analysed the effect of removing the APC/C subunit cdc27 in *bub3* mutant cells. It has recently been shown that in *Drosophila*, the APC/C subunit cdc27 is required for the degradation of cyclin B but not of securin (another APC/C substrate), as mutations in *cdc27* mutant neuroblasts or depletion of cdc27 by RNAi in S2 cells, results in cells with high levels of cyclin B and separated sister chromatids (Deak et al., 2003; Huang and Raff, 2002). Accordingly, mutations in the *bub3* and *cdc27* genes would be predicted to have opposite effects on the accumulation of cyclin B and the combination of the two mutations might even lead to normal mitotic entry. We therefore measured cyclin B levels in single (*bub3*^{1} or *cdc27*) and double (*bub3*^{1}*;cdc27)* mutant cells after incubation in colchicine (Fig. 5A,B and supplementary material Table S4). The results show that *cdc27* mutant cells have significantly higher levels of cyclin B both in G2 and mitosis than do control wild-type cells, in agreement with the phenotype previously described for this mutant (Deak et al., 2003). As expected, accumulation of cyclin B in double mutant cells (*bub3*^{1}*; cdc27*) during G2 is not significantly different from wild-type controls and it is higher than in *bub3*^{1} cells (Fig. 5B). These results support the hypothesis that the inability to accumulate normal levels of cyclin B after depletion of Bub3 is mediated by the APC/C.

Next, we analysed several mitotic parameters in single (*bub3*^{1} or *cdc27*) and double (*bub3*^{1}*; cdc27*) mutant cells after spindle damage induced by incubating the cells in colchicine (Fig. 5C,D and supplementary material Table S5). Under these conditions, mutant *cdc27* neuroblasts arrest in mitosis with well-condensed chromosomes and unseparated sister chromatids resulting in an increased mitotic index when compared to the wild-type control. This behaviour is due to the additive effect of the mutation in the APC/C subunit and the checkpoint-dependent arrest induced by spindle damage (Fig. 5C). In neuroblasts mutant for both *bub3*^{1} and *cdc27,* the percentage of cells in mitosis is increased relative to *bub3*^{1} alone. This result shows that the premature mitotic exit characteristic of *bub3*^{1} mutant cells is dependent on APC/C activity. Nevertheless, the mitotic index of double mutant cells (*bub3*^{1} and *cdc27*) is significantly lower than that seen in wild-type cells. This difference relative to control cells is most likely explained by premature mitotic exit due to the absence of an effective checkpoint response when Bub3 activity is absent, coupled with the fact that cdc27 does not seem to be required for APC/C-mediated securin degradation (data not shown). Finally, we observed that the frequency of cells in prophase in double mutant cells is indistinguishable from wild-type controls, suggesting that the double mutant transits normally through this early stage of mitosis (Fig. 5D). To rule out the possibility that cyclin B levels could be regulated by a mechanism other than APC/C-driven proteolysis, we overexpressed a non-degradable form of cyclin B (Wakefield et al., 2000) in *bub3*^{1} mutant neuroblasts using the GAL4/UAS system. The results show that stabilization of cyclin B in *bub3*^{1} mutant cells results in an increase in the mitotic index to values similar to those observed in control cells (Fig. 5E). Taken together, these results indicate that Bub3 appears to negatively regulate APC/C activity during the G2-M transition, allowing the accumulation of sufficient cyclin B for timely progression through the early stages of mitosis.

Analysis of cyclin A accumulation during the G2-M transition in Bub3-depleted cells

The results described above suggest that Bub3 is required for normal accumulation of cyclin B before and during mitosis. However, cyclin A is also required to promote mitotic entry in *Drosophila* (Parry and O'Farrell, 2001; Su, 2001). Cyclin A accumulates during S phase and G2 and it is degraded by the APC/C prior to the degradation of cyclin B as cells progress through early stages of mitosis. However, in contrast to cyclin B, cyclin A levels are not stabilized by the spindle damage-associated checkpoint response (Geley et al., 2001; Kaspar et al., 2001; Whitfield et al., 1990). In order to determine if Bub3 is also required to promote accumulation of cyclin A, we analysed its levels during cell cycle progression in Bub3-depleted cells. The centrosomal marker γ-tubulin was used to distinguish cells in G1/S or G2. The results show that although cyclin A accumulates from G1 to G2 in control cells (Fig. 6A,B and supplementary material Table S6) and can still be detected in some early mitotic cells (data not shown), cyclin A fails to accumulate and can hardly be detected in cells depleted for Bub3. Analysis of cyclin A accumulation in *bub3*^{1} homozygous mutant neuroblasts gave very similar results (data not shown). These observations further support the role of

Bub3 as a negative regulator of the APC/C during G2 and mitosis.

Analysis of cyclin B accumulation in *bubR1*^{1} mutant cells

Unlike other checkpoint proteins like Mad2 or BubR1, Bub3 has never been found to interact directly with the APC/C or with its activator Cdc20 (Fang, 2002; Fang et al., 1998; Wassmann and Benezra, 1998; Wu et al., 2000). Thus, we were interested to determine if other proteins that interact simultaneously with Bub3 and Cdc20 or APC/C subunits could mediate Bub3-dependent APC/C inhibition. BubR1 is, at first glance, a good candidate to perform this function as it has been found in an interphase high molecular weight complex (together with Bub3) that is able to inhibit the APC/C (Sudakin et al., 2001; Tang et al., 2001). Accordingly, we tested whether mutations in *bubR1* could affect cyclin B accumulation in G2 or mitosis (Fig. 7). Wild-type or *bubR1*^{1} third larval neuroblasts were incubated in colchicine and immunostained to reveal the level of chromatin condensation and cyclin B. Analysis of control cells shows that we could identify cells with no cyclin B and no chromosome condensation (classified as G1/S); cells with cyclin B levels but no visible chromatin condensation (classified as G2); and cells with high levels of cyclin B and well-condensed chromosomes (classified as mitotic), as expected for normal cyclin B accumulation. Similarly, we could detect *bubR1*^{1} mutant neuroblasts in G1 and also in G2 (Fig. 7A) with normal levels of cyclin B (Fig.7B). However, mitotic cells showed significantly lower levels of cyclin B (Fig. 7A,B) consistent with its known function in the mitotic checkpoint response. These results show that the pattern of cyclin B accumulation in the absence of *bubR1*^{1} is significantly different from that of *bub3*^{1} mutant cells (see supplementary material Fig. S1). Therefore, these data suggest that accumulation of cyclin B during G2 and early mitosis requires Bub3 independently of its interaction with BubR1.

Discussion

Mitotic checkpoint proteins are essential inhibitors of the metaphase-anaphase transition as they ensure that errors in the interactions between the spindle and the kinetochores can be corrected prior to exit from mitosis. Here we show that apart from its essential role in the checkpoint, Bub3 is also required during the G2/M transition and prophase to allow normal accumulation of mitotic cyclins presumably by regulating the activity of the APC/C. In the absence of Bub3, cells are unable to arrest in response to spindle damage and also progression through early stages of mitosis is delayed owing to significantly lower levels of cyclins A and B.

In order to study the role of Bub3 during mitosis we identified and characterized *bub3*^{1}, the first mutant allele of the gene in *Drosophila*. Analysis of *bub3*^{1} mutant cells indicates that as in other systems (Kalitsis et al., 2000), *bub3* is an essential gene. The *bub3*^{1} mutant allele appears to be hypomorphic as hemizygous neuroblasts and S2 cells depleted of Bub3 by RNAi show a more severe phenotype than *bub3*^{1} homozygous mutant cells. Also, as previously shown for other organisms (Babu et al., 2003; Campbell and Hardwick, 2003; Kalitsis et al., 2000), we show that in *Drosophila*, *bub3* is required for checkpoint-dependent mitotic arrest as its loss either by mutation or by RNAi causes PSCS, abnormal anaphase organization, significant aneuploidy and inability to arrest in mitosis after spindle damage.

In vivo analysis of cell division in Bub3-depleted cells reveals that this checkpoint protein could be required for the normal timing of mitosis. Using S2 cells stably expressing GFP-tubulin we find that after Bub3 depletion, mitosis (from NEBD to anaphase onset) is significantly faster than in control cells. This is at odds with recently published results where it was shown that in HeLa cells stably expressing H2B-GFP, Bub3-depleted cells enter anaphase with misaligned chromosomes but the timing between NEBD and anaphase onset is not altered (Meraldi et al., 2004). The reason for this discrepancy is not clear and we can only attribute it to a species-specific requirement for Bub3 during mitosis.

More significantly, our data revealed that cell cycle progression after *bub3* mutation or depletion is characterized by a high frequency of cells in prophase, suggesting a slower progression through the early stages of mitosis. Live analysis of Bub3-depleted cells confirmed these results. This delay in prophase appears to result from a defective accumulation of cyclins in both interphase and mitotic cells. Indeed, if we stabilize cyclin B in *bub3*^{1} mutant cells by a mutation in the gene for the APC/C subunit *cdc27* or through expression of a stable form of cyclin B, the mitotic index is increased and *bub3*^{1} mutant cells transit normally through early stages of mitosis. These results also suggest that the defective accumulation of cyclins in *bub3*^{1} mutant cells is likely to be APC/C dependent, suggesting that Bub3 is able to regulate APC/C activity well before its established role in the mitotic checkpoint response during prometaphase.

Bub3 has never been shown to bind either the APC/C or cdc20 directly. Therefore, it is possible that Bub3 affects APC/C activity through one of its binding partners, for example BubR1. However, the analysis of mitotic progression of *bub3*^{1} mutant cells causes a very different mitotic phenotype from that caused by mutations in *bubR1* (Basu et al., 1999) (see also Logarinho et al., 2004). Cells mutant for *bubR1* enter prophase normally but progress into anaphase as soon as the nuclear envelope breaks down, even before the completion of chromosome condensation, resulting in chromosome breakage and apoptosis. None of these phenotypes is observed after mutation of *bub3* or depletion of the Bub3 protein in S2 cells. These cells show significant aneuploidy and undergo premature mitotic exit, but with properly condensed chromosomes and showing no signs of apoptosis. Furthermore, the analysis of Bub3-depleted cells showed that the majority of the cells are delayed in prophase because they display mitosis-specific phosphorylation of histone H3 and retain an intact nuclear envelope. Although classified as prophase, only half of these cells show matured asters, a cytoplasmic event that should have taken place as cells enter mitosis. These results suggest that after Bub3 depletion, nuclear and cytoplasmic events can uncouple, an observation that is in agreement with a reduced activity of the cyclin/cdk complexes in the cytoplasm. A correlation between cyclin A and cyclin B dependent kinases and formation of the mitotic spindle is well established. It has been shown that cyclin A-dependent kinase activity increases the microtubule nucleating activity of centrosomes (Buendia et al., 1992). On the other hand, the reorganization of microtubules that ultimately leads to mitotic

spindle assembly seems to involve both cyclin A- and cyclin B-dependent kinase activities (Verde et al., 1992). Furthermore, it has been recently proposed that centrosome nucleated microtubules, at the prophase-prometaphase transition, promote tension when attached to the nuclear envelope and induce tearing of the nuclear lamin, thus promoting nuclear envelope invagination, permeabilization and eventually NEBD (Beaudouin et al., 2002). This model could explain how mitotic spindle formation and nuclear disassembly are two highly coordinated processes. Furthermore, in vivo studies in *Drosophila* embryos have shown that APC/C subunits, cdc27 and cdc16, accumulate at the nuclear envelope region during interphase and are only enriched in the nuclear area as cells enter prophase and NEBD takes place (Huang and Raff, 2002). Thus, the integrity of the nuclear envelope appears to establish a barrier between the nucleus and the cytoplasm during early stages of mitosis. Uncoupling of mitotic processes and delayed prophase may explain why *bub3*^{1} mutant cells undergo mitosis with properly condensed chromosomes.

It is widely accepted that during mitosis APC/C activity is suppressed by the checkpoint proteins as long as there is one kinetochore that is unattached to the spindle or that is not otherwise under tension (Rieder et al., 1995; Rieder et al., 1994). According to this model, checkpoint proteins including Bub1, BubR1, Bub3 and Mad2 are recruited to unattached kinetochores where specific protein complexes are produced that directly or indirectly inhibit APC/C activity (Chen et al., 1998; Martinez-Exposito et al., 1999; Shah and Cleveland, 2000; Skoufias et al., 2001). However, our results show that Bub3 appears to be required for inhibition of the APC/C independently of its localization to kinetochores as it only localizes to kinetochores during mitosis. Recently published results also suggest that multiprotein complexes, including Bub3-BubR1, Bub3-Mad2 or Bub3-BubR1-Mad2, that inhibit the APC/C can form in the absence of kinetochores (Sudakin et al., 2001; Tang et al., 2001). These results establish a possible mechanistic basis for the action of checkpoint proteins as regulators of APC/C activity independent of their kinetochore localization. Tight regulation of the APC/C activity ensures sequential destruction of APC/C substrates and the correct timing of mitotic events. During interphase, APC/C activity is regulated by Emi1, most probably by preventing binding of substrates to the APC/C (Reimann et al., 2001b). During G1/S, Emi1 blocks APC/C^{Cdh1} activity, allowing cyclin A accumulation and thus promoting G1/S transition (Reimann et al., 2001b). During G2 and early prophase, Emi1 is able to inhibit Cdc20, thereby promoting cyclin B accumulation and mitotic progression (Reimann et al., 2001a). Degradation of Emi1 occurs during prophase releasing APC/C inhibition (Margottin-Goguet et al., 2003). In this context, our data suggest that Bub3 could mediate APC/C inhibition before NEBD.

Recent results have suggested that more than one APC/C complex may be responsible for either sister chromatid separation or cyclin B destruction during mitosis (Huang and Raff, 2002). Our results on the mitotic behaviour and cyclin B accumulation in single (*bub3*^{1} and *cdc27*) and double (*bub3*^{1}*; cdc27*) mutant cells support this data and suggest that Bub3 might affect the activity of the different APC/C complexes. First, we show that incubation of *cdc27* mutant neuroblasts with colchicine leads to a mitotic arrest with unseparated sister chromatids and normal cyclin B levels, revealing a classical checkpoint response. Second, sister chromatid cohesion in *cdc27* mutants can be abolished by a mutation in *bub3,* showing that the APC/C-dependent separation of sister chromatids does not require cdc27. Third, cyclin B can be degraded during G2 or mitosis in the absence of *cdc27* when Bub3 is depleted or mutated. These observations are fully in accordance with previously published results showing that the APC/C subunits cdc16 and cdc27 have distinct locations during mitosis and that individual depletion of cdc16 or cdc27 proteins by RNAi leads to distinct mitotic phenotypes (Huang and Raff, 2002). Similarly, in yeast it has been shown that the APC/C subunit cdc27 is not required for the degradation of securin as overexpression of the cdk inhibitor Sic1 is sufficient to rescue the viability of cdc27 mutants (Thornton and Toczyski, 2003). Furthermore, mutations in the *Drosophila* homologue of APC5, another APC/C subunit, results in a phenotype similar in all respects to mutations in cdc27 including high levels of cyclin B and sister chromatid separation (Bentley et al., 2002). These data suggest that the activity of the different APC/C subunits may be required at different times during mitosis and at different locations within a cell, and may help to determine the specificity of the APC/C towards the substrates, thus reflecting differentially activated APC/C complexes.

Overall, our results suggest that checkpoint proteins might be required to restrain APC/C activity at multiple times during entry and progression through mitosis, revealing that what has been previously called the spindle assembly checkpoint is indeed a much broader regulatory mechanism that monitors events both before and during mitosis.

We thank C. F. Lehner for anti-cyclin B antibody, D. Glover for anti-cyclin A antibody, Ron Vale for the GFP-tubulin S2 cell line and J. Raff and J. Urban for fly stocks. Madalena Costa provided excellent technical assistance. C.S.L. is supported by a grant from FCT of Portugal. The laboratory of C.E.S. is supported by grants from FCT of Portugal and the TMR program of the EU. Work in the laboratory of M.L.G. is supported by NIH grant R01GM48430.

References

Amon, A. (1999). The spindle checkpoint. *Curr. Opin. Genet. Dev.* **9**, 69-75.

Babu, J. R., Jeganathan, K. B., Baker, D. J., Wu, X., Kang-Decker, N. and van Deursen, J. M. (2003). Rae1 is an essential mitotic checkpoint regulator that cooperates with Bub3 to prevent chromosome missegregation. *J. Cell Biol.* **160**, 341-353.

Basu, J., Logarinho, E., Herrmann, S., Bousbaa, H., Li, Z., Chan, G. K., Yen, T. J., Sunkel, C. E. and Goldberg, M. L. (1998). Localization of the Drosophila checkpoint control protein Bub3 to the kinetochore requires Bub1 but not Zw10 or Rod. *Chromosoma* **107**, 376-385.

Basu, J., Bousbaa, H., Logarinho, E., Li, Z., Williams, B. C., Lopes, C., Sunkel, C. E. and Goldberg, M. L. (1999). Mutations in the essential spindle checkpoint gene bub1 cause chromosome missegregation and fail to block apoptosis in Drosophila. *J. Cell Biol.* **146**, 13-28.

Beaudouin, J., Gerlich, D., Daigle, N., Eils, R. and Ellenberg, J. (2002). Nuclear envelope breakdown proceeds by microtubule-induced tearing of the lamina. *Cell* **108**, 83-96.

Bentley, A. M., Williams, B. C., Goldberg, M. L. and Andres, A. J. (2002). Phenotypic characterization of Drosophila ida mutants: defining the role of APC5 in cell cycle progression. *J. Cell Sci.* **115**, 949-961.

Brady, D. M. and Hardwick, K. G. (2000). Complex formation between Mad1p, Bub1p and Bub3p is crucial for spindle checkpoint function. *Curr. Biol.* **10**, 675-678.

Brand, A. H. and Perrimon, N. (1993). Targeted gene expression as a means

of altering cell fates and generating dominant phenotypes. *Development* **118**, 401-415.

Buendia, B., Draetta, G. and Karsenti, E. (1992). Regulation of the microtubule nucleating activity of centrosomes in Xenopus egg extracts: role of cyclin A-associated protein kinase. *J. Cell Biol.* **116**, 1431-1442.

Campbell, L. and Hardwick, K. G. (2003). Analysis of Bub3 spindle checkpoint function in Xenopus egg extracts. *J. Cell Sci.* **116**, 617-628.

Chen, R. H., Shevchenko, A., Mann, M. and Murray, A. W. (1998). Spindle checkpoint protein Xmad1 recruits Xmad2 to unattached kinetochores. *J. Cell Biol.* **143**, 283-295.

Deak, P., Donaldson, M. and Glover, D. M. (2003). Mutations in makos, a Drosophila gene encoding the Cdc27 subunit of the anaphase promoting complex, enhance centrosomal defects in polo and are suppressed by mutations in twins/aar, which encodes a regulatory subunit of PP2A. *J. Cell Sci.* **116**, 4147-4158.

Fang, G. (2002). Checkpoint protein BubR1 acts synergistically with Mad2 to inhibit anaphase-promoting complex. *Mol. Biol. Cell* **13**, 755-766.

Fang, G., Yu, H. and Kirschner, M. W. (1998). The checkpoint protein MAD2 and the mitotic regulator CDC20 form a ternary complex with the anaphase-promoting complex to control anaphase initiation. *Genes Dev.* **12**, 1871-1883.

Fraschini, R., Beretta, A., Sironi, L., Musacchio, A., Lucchini, G. and Piatti, S. (2001). Bub3 interaction with Mad2, Mad3 and Cdc20 is mediated by WD40 repeats and does not require intact kinetochores. *EMBO J.* **20**, 6648-6659.

Geley, S., Kramer, E., Gieffers, C., Gannon, J., Peters, J. M. and Hunt, T. (2001). Anaphase-promoting complex/cyclosome-dependent proteolysis of human cyclin A starts at the beginning of mitosis and is not subject to the spindle assembly checkpoint. *J. Cell Biol.* **153**, 137-148.

Hardwick, K. G., Johnston, R. C., Smith, D. L. and Murray, A. W. (2000). MAD3 encodes a novel component of the spindle checkpoint which interacts with Bub3p, Cdc20p, and Mad2p. *J. Cell Biol.* **148**, 871-882.

Harper, J. W., Burton, J. L. and Solomon, M. J. (2002). The anaphase-promoting complex: it's not just for mitosis any more. *Genes Dev.* **16**, 2179-2206.

Hendzel, M. J., Wei, Y., Mancini, M. A., van Hooser, A., Ranalli, T., Brinkley, B. R., Bazett-Jones, D. P. and Allis, C. D. (1997). Mitosis-specific phosphorylation of histone H3 initiates primarily within pericentromeric heterochromatin during G_2 and spreads in an ordered fashion coincident with mitotic chromosome condensation. *Chromosoma* **106**, 348-360.

Hoyt, M. A., Totis, L. and Roberts, B. T. (1991). S. cerevisiae genes required for cell cycle arrest in response to loss of microtubule function. *Cell* **66**, 507-517.

Hsu, J. Y., Reimann, J. D., Sorensen, C. S., Lukas, J. and Jackson, P. K. (2002). E2F-dependent accumulation of hEmi1 regulates S phase entry by inhibiting APC(Cdh1). *Nat. Cell Biol.* **4**, 358-366.

Huang, J. Y. and Raff, J. W. (2002). The dynamic localization of the Drosophila APC/C: evidence for the existence of multiple complexes that perform distinct functions and are differentially localized. *J. Cell Sci.* **115**, 2847-2856.

Jacobs, H. W., Knoblich, J. A. and Lehner, C. F. (1998). Drosophila Cyclin B3 is required for female fertility and is dispensable for mitosis like Cyclin B. *Genes Dev.* **12**, 3741-3751.

Kalitsis, P., Earle, E., Fowler, K. J. and Choo, K. H. (2000). Bub3 gene disruption in mice reveals essential mitotic spindle checkpoint function during early embryogenesis. *Genes Dev.* **14**, 2277-2282.

Kaspar, M., Dienemann, A., Schulze, C. and Sprenger, F. (2001). Mitotic degradation of cyclin A is mediated by multiple and novel destruction signals. *Curr. Biol.* **11**, 685-690.

Kimura, K., Hirano, M., Kobayashi, R. and Hirano, T. (1998). Phosphorylation and activation of 13S condensin by Cdc2 in vitro. *Science* **282**, 487-490.

Li, R. and Murray, A. W. (1991). Feedback control of mitosis in budding yeast. *Cell* **66**, 519-531.

Llamazares, S., Moreira, A., Tavares, A., Girdham, C., Spruce, B. A., Gonzalez, C., Karess, R. E., Glover, D. M. and Sunkel, C. E. (1991). polo encodes a protein kinase homolog required for mitosis in Drosophila. *Genes Dev.* **5**, 2153-2165.

Logarinho, E., Bousbaa, H., Dias, J. M., Lopes, C., Amorim, I., Antunes-Martins, A. and Sunkel, C. E. (2004). Different spindle checkpoint proteins monitor microtubule attachment and tension at kinetochores in Drosophila cells. *J. Cell Sci.* **117**, 1757-1771.

Margottin-Goguet, F., Hsu, J. Y., Loktev, A., Hsieh, H. M., Reimann, J. D. and Jackson, P. K. (2003). Prophase destruction of Emi1 by the SCF(betaTrCP/Slimb) ubiquitin ligase activates the anaphase promoting complex to allow progression beyond prometaphase. *Dev. Cell* **4**, 813-826.

Martinez-Exposito, M. J., Kaplan, K. B., Copeland, J. and Sorger, P. K. (1999). Retention of the Bub3 checkpoint protein on lagging chromosomes. *PNAS* **96**, 8493-8498.

Meraldi, P., Draviam, V. M. and Sorger, P. K. (2004). Timing and checkpoints in the regulation of mitotic progression. *Dev. Cell* **7**, 45-60.

Musacchio, A. and Hardwick, K. G. (2002). The spindle checkpoint: structural insights into dynamic signalling. *Nat. Rev. Mol. Cell Biol.* **3**, 731-741.

Parry, D. H. and O'Farrell, P. H. (2001). The schedule of destruction of three mitotic cyclins can dictate the timing of events during exit from mitosis. *Curr. Biol.* **11**, 671-683.

Peters, J. M. (2002). The anaphase-promoting complex: proteolysis in mitosis and beyond. *Mol. Cell* **9**, 931-943.

Platero, J. S., Hartnett, T. and Eissenberg, J. C. (1995). Functional analysis of the chromo domain of HP1. *EMBO J.* **14**, 3977-3986.

Reimann, J. D., Freed, E., Hsu, J. Y., Kramer, E. R., Peters, J. M. and Jackson, P. K. (2001a). Emi1 is a mitotic regulator that interacts with Cdc20 and inhibits the anaphase promoting complex. *Cell* **105**, 645-655.

Reimann, J. D., Gardner, B. E., Margottin-Goguet, F. and Jackson, P. K. (2001b). Emi1 regulates the anaphase-promoting complex by a different mechanism than Mad2 proteins. *Genes Dev.* **15**, 3278-3285.

Rieder, C. L., Schultz, A., Cole, R. and Sluder, G. (1994). Anaphase onset in vertebrate somatic cells is controlled by a checkpoint that monitors sister kinetochore attachment to the spindle. *J. Cell Biol.* **127**, 1301-1310.

Rieder, C. L., Cole, R. W., Khodjakov, A. and Sluder, G. (1995). The checkpoint delaying anaphase in response to chromosome monoorientation is mediated by an inhibitory signal produced by unattached kinetochores. *J. Cell Biol.* **130**, 941-948.

Shah, J. V. and Cleveland, D. W. (2000). Waiting for anaphase: Mad2 and the spindle assembly checkpoint. *Cell* **103**, 997-1000.

Skibbens, R. V. and Hieter, P. (1998). Kinetochores and the checkpoint mechanism that monitors for defects in the chromosome segregation machinery. *Annu. Rev. Genet.* **32**, 307-337.

Skoufias, D. A., Andreassen, P. R., Lacroix, F. B., Wilson, L. and Margolis, R. L. (2001). Mammalian mad2 and bub1/bubR1 recognize distinct spindle-attachment and kinetochore-tension checkpoints. *Proc. Natl. Acad. Sci. USA* **98**, 4492-4497.

Su, T. T. (2001). How, when and why cells get rid of cyclin A. *Curr. Biol.* **11**, R467-R469.

Sudakin, V., Chan, G. K. and Yen, T. J. (2001). Checkpoint inhibition of the APC/C in HeLa cells is mediated by a complex of BUBR1, BUB3, CDC20, and MAD2. *J. Cell Biol.* **154**, 925-936.

Tang, Z., Bharadwaj, R., Li, B. and Yu, H. (2001). Mad2-Independent inhibition of APCCdc20 by the mitotic checkpoint protein BubR1. *Dev. Cell* **1**, 227-237.

Taylor, S. S., Ha, E. and McKeon, F. (1998). The human homologue of Bub3 is required for kinetochore localization of Bub1 and a Mad3/Bub1-related protein kinase. *J. Cell Biol.* **142**, 1-11.

Thornton, B. R. and Toczyski, D. P. (2003). Securin and B-cyclin/CDK are the only essential targets of the APC. *Nat. Cell Biol.* **5**, 1090-1094.

Verde, F., Dogterom, M., Stelzer, E., Karsenti, E. and Leibler, S. (1992). Control of microtubule dynamics and length by cyclin A- and cyclin B-dependent kinases in Xenopus egg extracts. *J. Cell Biol.* **118**, 1097-1108.

Wakefield, J. G., Huang, J. Y. and Raff, J. W. (2000). Centrosomes have a role in regulating the destruction of cyclin B in early Drosophila embryos. *Curr. Biol.* **10**, 1367-1370.

Wassmann, K. and Benezra, R. (1998). Mad2 transiently associates with an APC/p55Cdc complex during mitosis. *Proc. Natl. Acad. Sci. USA* **95**, 11193-11198.

Weiss, E. and Winey, M. (1996). The Saccharomyces cerevisiae spindle pole body duplication gene MPS1 is part of a mitotic checkpoint. *J. Cell Biol.* **132**, 111-123.

Whitfield, W. G., Gonzalez, C., Maldonado-Codina, G. and Glover, D. M. (1990). The A- and B-type cyclins of Drosophila are accumulated and destroyed in temporally distinct events that define separable phases of the G_2-M transition. *EMBO J.* **9**, 2563-2572.

Wu, H., Lan, Z., Li, W., Wu, S., Weinstein, J., Sakamoto, K. M. and Dai, W. (2000). p55CDC/hCDC20 is associated with BUBR1 and may be a downstream target of the spindle checkpoint kinase. *Oncogene* **19**, 4557-4562.

Zachariae, W. and Nasmyth, K. (1999). Whose end is destruction: cell division and the anaphase-promoting complex. *Genes Dev.* **13**, 2039-2058.

Journal of Cell Science doi:10.1242/jcs.01602 Lopes et al., 2005
Supplementary material

Table S1. Quantification of mitotic parameters in wild-type and *bub3*^{1} mutant brains.

Genotype[a]	Time in colchicine (minutes)	Optical fields	Mitotic Figures	Prophase (number of cells)	%	Prometaphase (number of cells)	%	SCS (number of cells)	%	Mitotic Index
Oregon R	0	4478	3795	617	16.3	2366	62.3	812	21.4	0.85
	60	1798	1876	174	4.5	3675	94.8	27	0.7	2.16
***bub3*^{1}*/ bub3*^{1}**	0	2498	1390	211	15.2	833	59.9	117	24.9	0.56
	60	1102	493	70	14.2	348	70.6	75	15.2	0.45
bub3*^{1}*/ Df(3R)Dr-rv1	0	1936	1090	280	25.7	520	47.7	290	26.6	0.56
	60	1570	717	83	11.6	457	63.7	177	24.7	0.46

[a]Ten brains were scored for each genotype. Oregon R, wild-type control. SCS, sister chromatid separation.

Table S2. Quantification of cyclin B levels in cells with and without Bub3 after colchicine incubation.

	G1/S	G2	Mitosis
Oregon R	20.86 ± 3.16 (*n*=66)	33.66 ± 9.50 (*n*=162)	34.50 ± 9.15 (*n*=99)
bub3^{1}	21.98 ± 4.59 (*n*=42)	29.05 ± 17** (*n*=187)	28.00 ± 10.73*** (*n*=133)
Control	33.41 ± 9.13 (*n*=30)	65.41 ± 17.08 (*n*=50)	75.08 ± 20.04 (*n*=50)
Bub3 RNAi	35.25 ± 11.54 (*n*=46)	39.53 ± 11.50*** (*n*=72)	42.30 ± 9.45*** (*n*=26)

Oregon R, wild-type control. Values represent mean pixel intensity per cell ±s.d. *n*, number of cells scored. Cells from five different brains were analysed for each genotype. ***P*<0.005; ****P*<0.0005.

Table S3. Quantification of cyclin B levels in control and Bub3-depleted cells by RNAi.

	G1/S	G2
Control	17.098 ± 4.56 (*n*=251)	38.65 ± 12.89 (*n*=212)
Bub3 RNAi	16.48 ± 4.88 (*n*=210)	25.47 ± 6.32*** (*n*=169)

Values represent mean pixel intensity per cell ± s.d. *n*, number of cells scored.
***$P<0.0005$.

Table S4. Quantification of cyclin B levels in wild-type cells and after mutation of the APC/C subunit after colchicine incubation.

Genotype	G1/S	G2	Mitosis
Oregon R	19.04 ± 6.83 (*n*=166)	32.36 ± 15.39 (*n*=201)	35.34 ± 16.65 (*n*=177)
cdc27/cdc27	19.95 ± 4.36 (*n*=127)	51.17 ± 17.20*** (*n*=72)	75.03 ± 24.87*** (*n*=65)
cdc27;bub3^{1}/cdc27;bub3^{1}	16.39 ± 3.83 (*n*=100)	32.07 ± 14.7 (*n*=228)	28.49 ± 20.51* (*n*=98)

Oregon R, wild-type control. Values represent mean pixel intensity per cell ± s.d. *n*, number of cells scored. Cells from five different brains were analysed for each genotype. *P<0.05; ***P<0.0005.

Table S5. Quantification of mitotic parameters in neuroblasts mutated for *bub3* and the APC/C subunit *cdc27*.

Genotype	Optical Fields	Mitotic Figures	Prophase (number of cells)	%	Prometa-Metaphase (number of cells)	%	SCS (number of cells)	%	Mitotic Index
Oregon R	1798	3876	174	4.5	3675	94.8	27	0.7	2.16
cdc27⁻/cdc27⁻	1688	4660	336	7.2	4280	91.8	44	0.9	2.76
cdc27⁻ bub3¹ / ***cdc27⁻ bub3¹***	1202	1151	49	4.3	984	85.5	118	10.3	0.96
bub3¹/bub3¹	1102	493	70	14	348	70.6	75	15.2	0.45

Oregon R, wild-type control. At least five brains were scored for each genotype. SCS, sister chromatid separation.

Table S6. Quantification of cyclin A levels in control and cells depleted of Bub3 by RNAi.

	G1/S	G2
Control	23.29 ± 7.65 (*n*=50)	49.75 ± 26.03 (*n*=79)
Bub3 RNAi	5.84 ± 1.59*** (*n*=53)	8.65 ± 3.59*** (*n*=48)

Values represent mean pixel intensity per cell ± s.d. *n*, number of cells scored.
****P*<0.0005.

Table S7. Quantification of cyclin B levels in wild-type and *bubR1*^{1} mutant neuroblasts after colchicine incubation.

	G1/S	G2	Mitosis
Oregon R	20.86 ± 3.16 (*n*=66)	33.66 ± 9.50 (*n*=162)	34.50 ± 9.15 (*n*=99)
***bubR1*^{1}**	20.41 ± 6.79 (*n*=106)	33.07 ± 16.37 (*n*=161)	29 ± 14.87*** (*n*=47)

Oregon R, wild-type control. Values represent mean pixel intensity per cell ± s.d. *n*, number of cells scored. Cells from five different brains were analysed for each genotype. ***$P<0.0005$.